JOURNAL OF Materials CHEMISTRY

Structural and physical characterisation of transparent conducting pulsed laser deposited In_2O_3–ZnO thin films

Negar Naghavi,* Corinne Marcel, Loïc Dupont, Aline Rougier, Jean-Bernard Leriche and Claude Guéry

Laboratoire de Réactivité et Chimie des Solides, Université de Picardie Jules Verne, 33 rue St Leu, 80039 Amiens Cedex, France. E-mail: negar.naghavi@sc.u-picardie.fr

Received 15th March 2000, Accepted 7th July 2000
First published as an Advanced Article on the web 4th September 2000

Indium–zinc oxide thin films, with compositions ranging from In_2O_3 to ZnO, were prepared by pulsed laser deposition using a substrate temperature of 500 °C and an oxygen pressure of 10^{-3} mbar. X-Ray diffraction studies coupled with transmission electron microscopy revealed that the texture and the structure of the films are composition dependent with however a preferred orientation for all compositions, excluding In_2O_3 for consideration. As the Zn/(Zn + In) atomic ratio increased, the film structure evolved from cubic In_2O_3 to hexagonal ZnO *via* a hexagonal layered $Zn_kIn_2O_{k+3}$ structure. An average transmittance of 85–90% in the visible region was obtained for all films independently of the composition. The maximum conductivity ($\sigma = 1500$ S cm^{-1}) was reached for a film having an atomic ratio Zn/(Zn + In) = 0.5 (*i.e.* $Zn_2In_2O_5$).

1 Introduction

During the last decade, transparent conducting oxides (TCO) films have been used in a variety of optoelectronic devices such as displays, solar cells and electrochromic devices. At present, ITO (Sn doped indium oxide) is the most commonly used TCO material due to its excellent properties with a conductivity of 1000–5000 S cm^{-1} and an optical transparency of 85–95% in the visible region. However, in the search for lower cost transparent conducting oxides with similar or even better properties than ITO, a large number of studies have recently been devoted to new materials.[1–7] One of the promising systems is the indium–zinc oxide system. Moriga *et al.*[8] studied the structural and physical properties of phase relationships in bulk In_2O_3–ZnO, and revealed nine homologous compounds of $Zn_kIn_2O_{k+3}$ composition ($k = 3$, 4, 5, 6, 7, 9, 11, 13 and 15), where the highest conductivity and the lowest transparency were observed for $Zn_3In_2O_6$. However, the authors pointed out that, as the conductivity increases with decreasing k, a lower-order member of the series, $Zn_kIn_2O_{k+3}$ ($k = 1$ and 2), unstable at the bulk level, should have a higher conductivity than that of $Zn_3In_2O_6$. Therefore, high interest was devoted to the thin film route, which should be more suitable for the preparation of metastable phases.[9–13] In a recent paper, we showed using pulsed laser deposition that the growth conditions, leading to the highest conductivity of the $Zn_3In_2O_6$ composition, were an optimum oxygen pressure of 10^{-3} mbar and an optimum substrate temperature of 500 °C.[14]

In this paper, we report the study of indium–zinc oxide pulsed laser deposited films with compositions ranging from In_2O_3 to ZnO. The influence of the composition (*i.e.* the atomic ratio $x = Zn/(Zn + In)$) on the structural and physical properties of the films is discussed on the basis of what has been learnt from bulk studies.

2 Experimental

Indium–zinc oxide thin films were deposited on a 1 cm^2 glass substrate by pulsed laser deposition using a KrF excimer laser beam (Lambda Physik, Compex 102, $\lambda = 248$ nm) with a laser fluence of 1–2 J cm^{-2}. The base pressure in the chamber was of the order of 10^{-6} mbar. Deposition times were typically 40 min with a repetition rate of 10 Hz (0.16 to 0.23 Å per shot). The substrate temperature and the oxygen pressure were fixed at 500 °C and 10^{-3} mbar, respectively. The targets were pellets of ZnO and In_2O_3 mixtures in stoichiometric proportions. $Zn_kIn_2O_{k+3}$ ($3 \leqslant k \leqslant 15$) stable phases were obtained using the ceramic process reported by Moriga *et al.*[8] For the other mixtures, metastable in the bulk state, stoichiometric proportions of ZnO and In_2O_3 powders were heated for 5 days at 1250 °C. The targets had a density between 80 and 90% of the theoretical value.

The crystallinity of the films was examined by X-ray diffraction (XRD) with a Philips diffractometer model PW 1710 ($\lambda_{CuK_\alpha} = 0.15418$ nm). The surface morphology and the composition of the films were investigated by scanning electron microscopy with a Philips XL 30 field emission gun (FEG) coupled to an Oxford Link instrument for energy-dispersive X-ray spectroscopy (EDS). In the following the Zn/(Zn + In) atomic ratio is described as x. Transmission electron microscopy was carried out using a JEOL 2010 microscope.

Optical transmission spectra in the UV-visible and near infrared regions (250–2500 nm) were obtained using a Varian double beam, UV-Vis-NIR spectrometer "CARY-5E". The thickness of the film was determined by profilometry, using a Dektak^{3}St instrument. The obtained values were in the 400 to 550 nm range.

The conductivity of the samples was taken as the inverse of the resistivity (ρ) which was determined using the four-point probe method with applied currents of 1 to 50 mA. DC voltages and currents were measured with a multimeter (Keithley, 175A). The sheet resistivity was calculated as

$$\rho_s = \left(\frac{V}{I}\right) C\left(\frac{a}{d}, \frac{d}{s}\right)$$

and the resistivity as $\rho = \rho_s W$, where ρ is the resistivity, ρ_s is the sheet resistivity, V is the voltage, I is the current, W is the film thickness, a and d are the sample lengths (in our case $a = d$), s is the electrode spacing, and $C\left(\frac{a}{d}, \frac{d}{s}\right)$ is a correction factor accounting for the sample geometry.[15] Hall-effect measurements were carried out using the Van der Pauw method. In order to reject noise, which would hide the lowest mobility values, AC voltages and currents were measured with a PAR 124 type synchronized detector, while a 1.2 T magnetic field was applied through the square sample.

This journal is © The Royal Society of Chemistry 2000

3 Results and discussion

3.1 Influence of the composition on film structure and morphology

The study of the texture and the structure of the deposited films and their evolution as a function of Zn/(Zn + In) atomic ratio is important in better understanding the electrical and optical properties of these materials.

All films are dense and homogeneous and whatever the zinc content, the Zn/(Zn + In) atomic ratio is well preserved between the target and the films.

TEM micrographs revealed that films are polycrystalline and three different kinds of texture were observed depending on the composition. As shown in Fig. 1a, for very low amounts of zinc ($x = 0.15$), films are formed with particles having a cubic shape, and sizes ranging from 50 to 100 nm. As the zinc content increases ($x > 0.30$) the texture of the films evolves to a fiber type layered structure (Fig. 1b), which is maintained for all the compositions ranging from $x \approx 0.33$ to $x \approx 0.90$. For very high zinc contents (Fig. 1c), a columnar structure is observed. Such a columnar structure has been previously identified for Al-doped zinc oxides having a hexagonal ZnO wurtzite structure.[16]

X-Ray diffraction studies show that whatever the composition the films are textured, and their structure is composition dependent. The XRD patterns exhibit sharp and strong reflections ascribable to a cubic In_2O_3 structure at very low zinc amounts and to a hexagonal ZnO structure at very high zinc amounts, respectively (Fig. 2b and c). A pure In_2O_3 film presents two intense peaks located at 4.13 Å ($2\theta = 21.5°$) and 2.92 Å ($2\theta = 30.6°$), which by reference to its crystalline structure can be assigned to the (211) and (222) reflections, respectively (Fig. 2a). Pure ZnO thin films are *c*-axis oriented, and only two diffraction peaks located at 2.6 Å ($2\theta = 34.4°$) and 1.3 Å ($2\theta = 72.6°$) assigned to the (002) and (004) reflections of ZnO wurtzite structure are observed. The addition of a small amount of zinc oxide (*i.e.* $x = 0.15$) to pure In_2O_3 leads to a strong enhancement of the (222) reflection (Fig. 2b). For a Zn/(Zn + In) ratio greater than 0.30, only the intense reflection together with two extra weak and broad ones remain (* in Fig. 3a). As the amount of zinc is further increased, the intense reflection shifts to higher 2θ values, while remaining between the In_2O_3 (222) and ZnO (002) peak positions (Fig. 3b). Indeed the *d*(222) of In_2O_3 and the *d*(002) of ZnO correspond to the distance between two close packed layers in each of the two oxides. For films compositions between $0.60 \leqslant x \leqslant 0.88$ a comparison between the X-ray patterns of the films and the corresponding powders for $Zn_kIn_2O_{k+3}$ ($3 \leqslant k \leqslant 15$) reveals that reflections observed in the as-deposited film can be assigned to the (00*l*) reflection position of the corresponding powder, suggesting a *c*-axis orientation. Li *et al.*[17] showed that the basic structure of hexagonal $Zn_kIn_2O_{k+3}$ powders consists of InO_2^- layers interleaved with $InZn_kO_{k+1}^+$ (In/Zn–O layer) layers along the *c*-axis. In this composition range ($0.60 \leqslant x \leqslant 0.88$), the *d*-spacing deduced from the intense reflection of the X-ray pattern matches well with two In/Zn–O interlayer distances calculated from the $Zn_kIn_2O_{k+3}$ ($3 \leqslant k \leqslant 15$) structure of the corresponding powders. In summary, XRD information suggests that the structure of the In_2O_3–ZnO thin films evolves from cubic In_2O_3 to hexagonal ZnO *via* a layered hexagonal $Zn_kIn_2O_{k+3}$ domain.

To confirm the evolution of the structure in the films, high-resolution transmission electron microscopy (HRTEM) experiments on the complete system were investigated.[18] Briefly, these measurements confirm that the microstructure of the films is strongly composition dependent. The presence of a layered $Zn_kIn_2O_{k+3}$ type structure domain (with *k* ranging from 1 to 15 and even more) for films with $0.33 < x < 0.90$ compositions was revealed. Each grain or fiber is subdivided into smaller regions

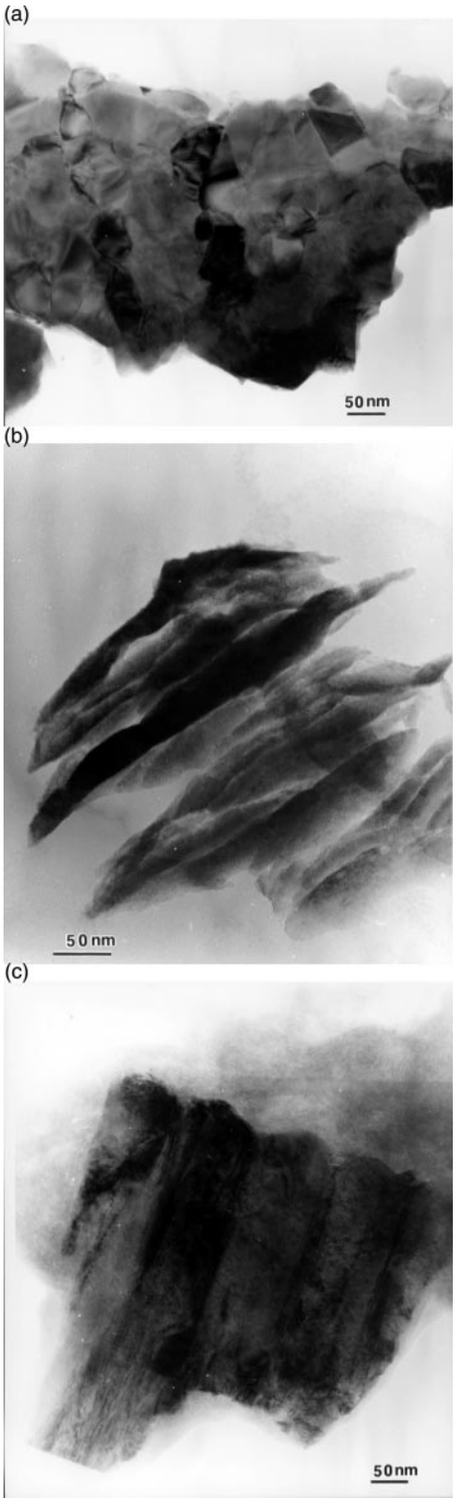

Fig. 1 TEM micrographs of indium–zinc oxide thin films with a) Zn/(Zn + In) = 0.15, b) Zn/(Zn + In) = 0.60 and c) Zn/(Zn + In) = 0.98.

or domains. These domains are all polytype each having a layered structure formed of two InO_2^- layers interleaved with ($k+1$) In/Zn–O layers but the *k* value might be different between various domains. Global observation shows that those domains are randomly distributed within the film. Nevertheless, for each film with a nominal Zn/(Zn + In) composition the corresponding $Zn_kIn_2O_{k+3}$ phase remains dominant. The formation of a multitude of polytype domains within films results in a broadening of the X-ray diffraction peaks. It is interesting to note that, for $x = 0.50$, a layered $Zn_2In_2O_5$ structure, metastable in bulk, is observed for the first time. On the other hand, for the composition corresponding to $k = 1$

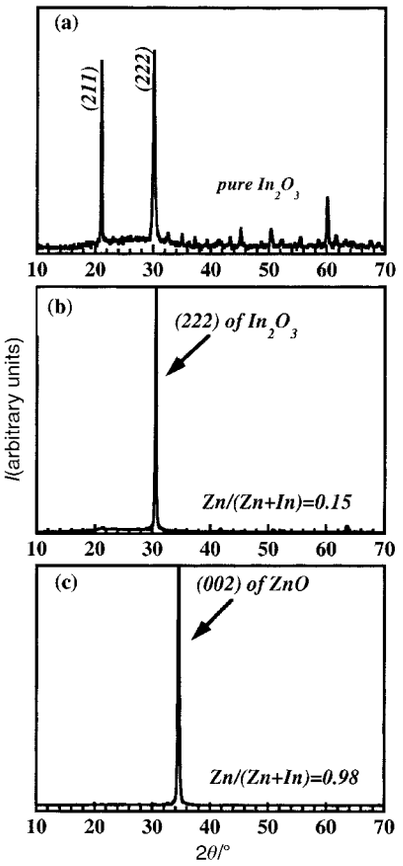

Fig. 2 Thin film X-ray diffraction patterns of a) pure In_2O_3, b) indium–zinc oxide with Zn/(Zn + In) = 0.15 and c) indium–zinc oxide with Zn/(Zn + In) = 0.98.

($x = 0.33$), a mixture of a layered $ZnIn_2O_4$ structure and pure In_2O_3 is observed.

3.2 Influence of the composition on the physical properties of the films

For transparent conducting oxides, good electrical properties can be achieved but often at the expense of transmission. The mechanisms of optical transmission and electrical conduction are interdependent. In this section, the optical properties of the films are first discussed, followed by a discussion on the variation of the electrical properties.

3.2.1 Optical properties. All the films are colourless independent of their composition. Fig. 4 shows the transmission spectra in the UV-visible and near infrared (300–2500 nm) for $x \leqslant 0.66$. In the visible region, the transmittance remains close to 85–90%, whatever the zinc content. The main difference takes place in the near infrared region where, for any $x > 0.60$ composition, the transmittance is very similar to the $x = 0.66$ whereas for low zinc contents noticeable changes are observed. It is well known that in the case of heavily doped semiconductors the Drude model, based on the Free Electron Theory, can be applied to describe the optical properties of thin films.[19] In the near infrared region, the transmittance drops as a result of free electron absorption. Briefly, in this region, the decrease in the transmittance is associated with an absorption peak followed by an increase in the reflectivity corresponding to the plasma frequency ω_p that can be expressed as

$$\omega_p^2 = (4\pi ne^2/m^*\varepsilon_\infty) \quad (1)$$

where n is the nearly free carrier concentration, m^* the effective mass, e the elementary charge and ε_∞ the dielectric constant extrapolated towards high energy. Therefore, as a first

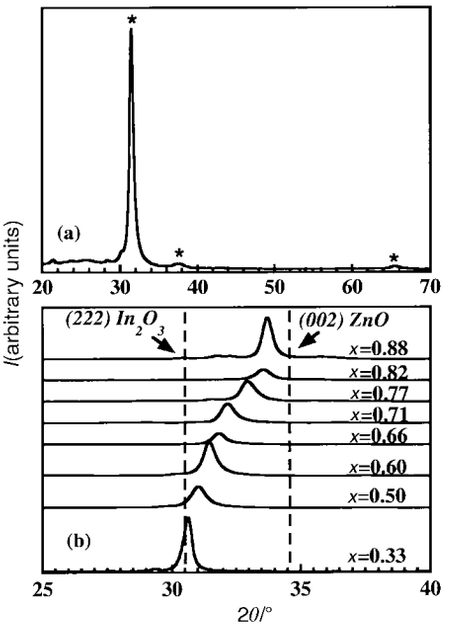

Fig. 3 X-Ray diffraction patterns of indium–zinc oxide thin films with a) Zn/(Zn + In) = 0.66 corresponding to a $Zn_3In_2O_6$ composition and b) x = Zn/(Zn + In) compositions varying from 0.33 to 0.88 corresponding to $Zn_kIn_2O_{k+3}$ ($k = 1, 2, 3, 4, 5, 7, 11$ and 15).

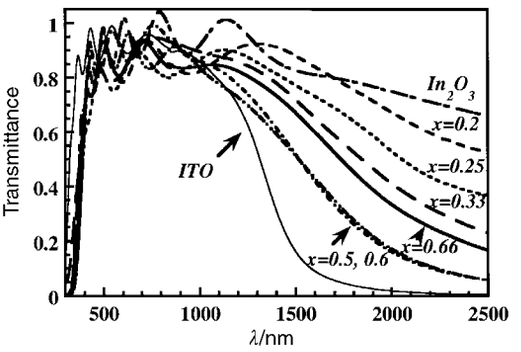

Fig. 4 Optical transmission spectra of ITO and indium–zinc oxide thin films with x = Zn/(Zn + In) compositions varying from 0 to 0.66.

approximation as the zinc content increases to a ratio of $x = 0.60$, the lowering of the transmittance level in the near infrared region may be associated with an increase in the carrier concentration (n). This tendency was indeed confirmed from Hall-effect measurements as reported in Fig. 5. The average

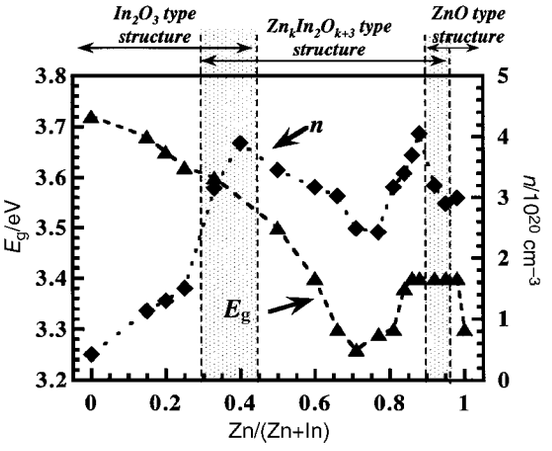

Fig. 5 Variation of the carrier concentration (n) (◆) and the optical band-gap (E_g) estimated from optical spectra (▲) as a function of the Zn/(Zn + In) ratio and the structure evolution.

transparency window of In_2O_3–ZnO is considerably greater than that of typical ITO films. Indeed, in our system, the free carrier concentration is in the order of 10^{20} cm^{-3}, instead of 10^{21} cm^{-3} for ITO. Thus, a lower carrier concentration shifts the IR transmittance cutt-off to higher wavelength, leading to a widening of the optical window.

In the UV region, the transmission falls very sharply due to the onset of fundamental absorption. The marked decrease in the transmittance at wavelengths shorter than about 400 nm is ascribed to the band-gap energy (E_g), the values of which, given in Fig. 5, are determined by extrapolation of the linear portion of α^2 *versus* $h\nu$, where α is the absorption coefficient. Herein we only consider direct transitions occurring within polycrystalline materials under the parabolic band hypothesis. Indeed, pure In_2O_3 and pure ZnO oxides have both intrinsic band-gaps (3.7 and 3.3 eV respectively) where the main interband transition is direct. For $x<0.70$, the band-gap continuously decreases from 3.70 to 3.25 eV and then slightly increases. For high zinc content ($x>0.80$), regardless of the composition, the band-gap remains constant at about 3.4 eV. In the very high zinc content region, the In_2O_3–ZnO thin films should be better described as indium doped zinc oxide. Therefore, the optical band-gap value, slightly higher than that of ZnO (3.3 eV), would result from a band filling effect associated with a blue shift of the absorption edge known as the Moss–Burstein shift.[20] Burstein has reported that the increase in the optical band-gap with an increase in the electron concentration is related to the Fermi level being raised within the conduction band in degenerate semiconductors. In summary, the optical band-gap is shifted towards short wavelengths with high carrier density values. A correlation between the band-gap energy and the electron concentration reveals that for $x<0.4$ the Moss–Burstein theory cannot be applied, in the sense that the carrier concentration increases while the optical band-gap continuously decreases (Fig. 5). At this stage, we can assume that Zn^{2+} ionized impurities would act as electron traps in the In_2O_3 lattice; when the content of these defects increases, the corresponding localized levels within the band-gap would overlap the bottom of the conduction band, thus reducing the optical band-gap, and releasing the trapped electrons. Moreover, one can suppose that the decrease in the band-gap energy can be tied to the evolution of the In_2O_3 band structure towards a new band structure specific to $Zn_kIn_2O_{k+3}$ materials. To complete this optical study, a model of the optical spectra is being investigated, and will be reported in the near future. In general all the In_2O_3–ZnO thin films have a smaller band-gap than the well known ITO ($E_g \approx 4.2$ eV), which permits absorption of more undesirable ultraviolet radiation.

3.2.2 Electrical properties. Hall effect measurements reveal that considering the obtained carrier concentrations ($n>10^{20}$ cm^{-3}) all films are degenerate, and according to Hall effect deviation they are n-type semiconductors. Moreover the electrical conductivity decreases as a function of temperature, exhibiting metal-like charge transport behavior for all films, which is typical of degenerate semiconductor materials. The n-type conduction is probably due to free electrons originating from oxygen vacancies caused by the very low oxygen pressure during the deposition (10^{-3} mbar). Fig. 6 presents the conductivity (σ), carrier concentration (n) and Hall mobility (μ) of our films *versus* Zn/(Zn+In) content. Compared to pure In_2O_3, a slight addition of ZnO to In_2O_3 leads to a decrease in both the mobility and the conductivity, followed by an increase to reach a maximum conductivity value of 1500 S cm^{-1}, a mobility (μ) of 27 cm^2 V^{-1} s^{-1} and a carrier concentration (n) of 3.4×10^{20} cm^{-3}, for the $x=0.50$ ratio, which is usually referred to as "$Zn_2In_2O_5$". These values can be

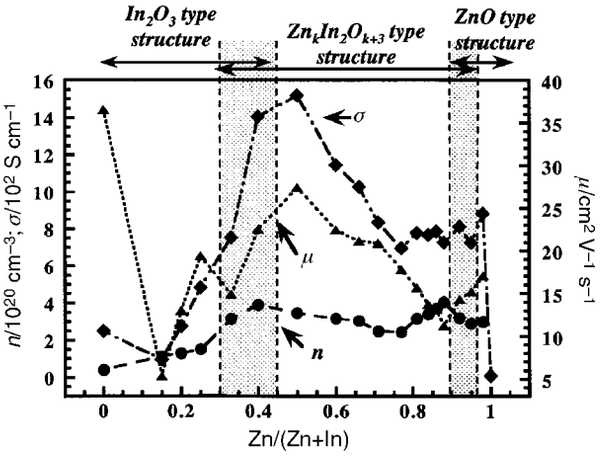

Fig. 6 Variation of the conductivity (σ) (◆), the carrier concentration (n) (●), and the mobility (μ) (▲) as a function of Zn/(Zn+In) ratio and the structure evolution.

favourably compared with the highest σ values of 1000 S cm^{-1} obtained for a $Zn_{0.66}In_2O_{3.66}$ film deposited by MOCVD,[11] and of 2500 S cm^{-1} for a $Zn_2In_2O_5$ composition deposited by magnetron sputtering.[21]

The increase in the conductivity may be achieved by increasing either the carrier concentration or the carrier mobility. In our case the carrier concentration (n) is mainly influenced by oxygen vacancies and the mobility (μ) may be influenced by the change in texture or structure of the films. For $x<0.50$, excluding pure In_2O_3, both the mobility and the carrier concentration increase as the zinc content increases. The initial enhancement of conductivity may be understood based on the evolution of the film texture, which evolves from a grain texture to a fibre texture, as the zinc content increases, thus improving the mobility.

For $0.50\leqslant x<0.70$ ($2\leqslant k\leqslant 7$) the conductivity as well as the mobility and the carrier concentration slightly decrease but for higher zinc contents ($0.70<x<0.90$ or $7\leqslant k\leqslant 15$) the conductivity becomes stable instead of continuously decreasing as expected, which is mainly due to an increase in the carrier concentration combined with a continuous mobility drop. This carrier concentration trend can be explained as follows. For $x\leqslant 0.90$ the low oxygen deposition pressure (10^{-3} mbar) may have an enhanced reduction effect for the high zinc content domain, increasing the carrier concentration and preventing the decrease in conductivity within the composition. This tendency will be totally consistent with the results of reduction experiments previously performed in the $Zn_kIn_2O_{k+3}$ bulk system.[8] Indeed, the reduction of $Zn_kIn_2O_{k+3}$ powders in forming gas leads to an increase in the conductivity with a stronger effect for higher k values. Moreover, the mobility decrease in the $0.50\leqslant x\leqslant 0.90$ range may be caused by an enhancement of multiple polytype domain numbers as the Zn/(Zn+In) ratio increases, leading to the formation of additional domain boundaries. However, as we explained in the previous section, for each film in this range of compositions ($0.50<x<0.90$) the corresponding $Zn_kIn_2O_{k+3}$ phase remains dominant, which enables a comparison between the bulk and film properties. For bulk materials the mobility of $Zn_kIn_2O_{k+3}$ powders was found to decrease as k increases;[8] however, no real explanation was given for such a composition driven mobility variation.

For very high zinc amounts, $x\geqslant 0.90$, in comparison to pure ZnO, the conductivity increased noticeably. Indium could act as a dopant with respect to ZnO, providing free electrons in the films (*i.e.* increase of n) and leading to an improvement of the electrical properties in agreement with previous work.[20] The slight mobility decrease for indium doped zinc oxide as the indium content increases ($0.90\leqslant x\leqslant 1$) may be due to the fact

that indium atoms in the films not only produce conduction electrons, but also deform the crystal structure. Defect scattering in crystals usually results in a lower value of mobility.

4 Conclusion

High quality In_2O_3–ZnO thin films with compositions ranging from In_2O_3 to ZnO were prepared by pulsed laser deposition. The best conductivity was found to be 1500 S cm^{-1} for a $Zn_2In_2O_5$ composition with a band-gap of about 3.5 eV and a transmission of 90% in the visible region. The optical properties are slightly dependent on the film composition in the visible region and the transmittance remains between 85 and 90%. On the other hand, the structure and morphology of the films depend on the composition. The structure of the films gradually evolves from a cubic In_2O_3 structure to a hexagonal layered phase similar to $Zn_kIn_2O_{k+3}$ materials, and exhibit a hexagonal ZnO structure for very high zinc content. In this last region, indium oxide acts as a dopant for ZnO and both the conductivity and the band-gap remain stable at about 800 S cm^{-1} and 3.4 eV, respectively. For all compositions the optical window is wider than for the well-known ITO, however none of them allows the In_2O_3–ZnO film conductivity to reach that of ITO. Nevertheless, this study provides a better understanding of the relationship between the structural and physical properties in this system, therefore opening new possibilities for the selection of the right substituent so as to obtain other metal substituted indium–zinc oxide films, which could compete with ITO in terms of electrical conductivity.

Acknowledgements

The authors wish to thank J. M. Tarascon for helpful discussions as well as M. Hervieu and B. Mercey for their kind advice regarding HTREM measurements and J. Salardenne and G. Couturier for the perfomance of Hall-effect measurements.

References

1 G. B. Palmer, K. R. Poeppelmeier and T. O. Mason, *Chem. Mater.*, 1997, **9**, 3121.
2 Z. C. Jin, I. Hamberg and C. G. Granqvist, *J. Appl. Phys.*, 1988, **64**, 5117.
3 D. D. Edwards, T. O. Mason, F. Goutenoire and K. R. Poeppelmeier, *Appl. Phys. Lett.*, 1997, **70**, 1706.
4 R. Wang, L. L. H. King and A. W. Sleight, *J. Mater. Res.*, 1996, **11**, 1659.
5 X. Wu, T. J. Coutts and W. P. Milligan, *J. Vac. Sci. Technol. A*, 1997, **15**, 1057.
6 Z. Y. Ning, S. H. Cheng, S. B. Ge, Y. Chao, Z. Q. Gang, Y. X. Zhang and Z. G. Liu, *Thin Solid Films*, 1997, **307**, 50.
7 T. Minami, T. Kakumu and H. Sonohara, *Thin Solid Films*, 1995, **22**, 270.
8 T. Moriga, D. Edwards, T. O. Mason, G. B. Palmer, K. R. Poeppelmeier, J. Schindler, C. Kannewurf and I. Nakabayashi, *J. Am. Ceram. Soc.*, 1998, **81**, 1310.
9 T. Minami, T. Kakumu and S. Takata, *J. Vac. Sci. Technol. A*, 1996, **14**, 1704.
10 D. J. Goyal, C. Agashe, M. G. Takwale and V. G. Bhide, *J. Mater. Res.*, 1993, **8**, 1052.
11 A. Wang, J. Dai, J. Cheng, M. P. Chudzik, T. J. Marks, R. P. H. Chang and C. R. Kannewurf, *Appl. Phys. Lett.*, 1998, **3**, 327.
12 J. M. Phillips, R. J. Cava, G. A. Thomas, S. A. Carter, J. Kwo, T. Siegrist, J. J. Krajewski, J. H. Marshall, W. F. Peck Jr. and D. H. Rapkine, *Appl. Phys. Lett.*, 1994, **67**, 2248.
13 J. P. Zheng and H. S. Kwok, *Thin Solid Films*, 1993, **232**, 99.
14 N. Naghavi, A. Rougier, C. Marcel, C. Guéry, J. B. Leriche and J. M. Tarascon, *Thin Solid Films*, 2000, **360**, 233.
15 F. M. Smits, *Bell Syst. Tech. J.*, 1958, **37**, 711.
16 I. Sieber, N. Wanderka, I. Urban, I. Dörfel, E. Schierhorn, F. Fenske and W. Fuhs, *Thin Solid Films*, 1998, **330**, 108.
17 C. Li, Y. Bando, M. Nakamura and N. Kimizuka, *J. Electron Microsc.*, 1997, **46**, 119.
18 L. Dupont, C. Maugy, N. Naghavi, C. Guéry and J. M. Tarascon, unpublished work.
19 I. Hamberg and C. G. Granqvist, *J. Appl. Phys.*, 1986, **60**, 123.
20 R. Wang, L. L. H. King and A. Sleight, *J. Mater. Res.*, 1996, **11**, 1659.
21 T. Minami, H. Sonohara, T. Kakumu and S. Takata, *Jpn. J. Appl. Phys.*, 1995, **34**, L971.